ChemComm

Transformation of single MOF nanocrystals into single nanostructured catalysts within mesoporous supports: platform for pioneer Fluidized-Nanoreactor Hydrogen Carriers

Journal:	*ChemComm*
Manuscript ID	CC-COM-06-2018-004562.R1
Article Type:	Communication

Chemical Communication

COMMUNICATION

Transformation of single MOF nanocrystals into single nanostructured catalysts within mesoporous supports: platform for pioneer Fluidized-Nanoreactor Hydrogen Carriers

Received 00th January 20xx,
Accepted 00th January 20xx

DOI: 10.1039/x0xx00000x

www.rsc.org/

Ignacio Luz, Mustapha Soukri* and Marty Lail

Well-dispersed nanostructured catalysts along mesoporous materials have been systematically prepared via a novel multistep approach involving either the pyrolysis under nitrogen, the calcination under oxygen or the reduction under hydrogen of MOF nanocrystals decorated with transition metal complexes and previously confined within the mesoporous cavities via novel solid state synthesis. The resulting supported nanostructured catalysts can be composed by metals, metal oxides, heteroatom-doped carbons and combinations thereof depending on the transformation conditions. Pioneer concept of Fluidized-Nanoreactor Hydrogen Carriers has been first time proposed by using the resulting nanostructured catalysts within fluidized mesoporous silica.

MOFs have been widely used as versatile precursors for the preparation of catalytically active materials upon applying certain conditions, such as controlled pyrolysis under nitrogen, calcination under oxygen or reduction under hydrogen[1]. The versatility of MOFs as precursors is mainly due to their unique and highly tunable features, such as well-defined metal sites spaced by organic struts displayed along a crystalline structure with permanent porosity, which can play two simultaneous roles acting as template and precursor[2, 3]. Upon transformation, MOFs can lead to well-defined nanostructured catalytically active species, which are monodispersed within hierarchical scaffolds, depending on the conversion conditions, i.e., microporous metal oxide under oxidant conditions or microporous carbonaceous matrix under inert conditions. The resulting nanostructured catalysts can be composed by metals, metal oxides, heteroatom-doped carbon and combinations thereof[4].

The use of nano-sized MOF domains (5-50 nm) as precursor instead of bulkier particles can offer some advantages from the catalytic point of view after transformation, as they can lead to the isolation of a reduced number of metallic or metal oxide atoms, and even forming sub-nanometric crystalline domains or also denominated clusters[5]. However, the use of free-standing MOF nanocrystals as precursors is not yet proposed due to their poor stability under high temperatures that may promote their fusion into larger aggregates under the required transformation conditions, thereby leading to the same scenario than starting from bulkier MOF precursors. Therefore, novel synthetic routes are highly demanded to avoid MOF nanocrystals from sintering during high temperature treatments, thus paving the way to the development of new generation of MOF-derived nanostructured catalysts.

Our group has recently reported a general method for the selectively confinement of MOF nanocrystals within mesoporous materials (MPMs) via 'solid-state' synthesis[6]. This versatile approach provides high level of design over the resulting hybrid material formulation and nanoarchitecture, such as composition, loading and dispersion of the MOF guest as well as composition, pore size distribution and particle size of the mesoporous material host. MOF crystalline domains are always restricted to the dimensions delimited by the hosting cavity of the mesoporous material. In the same way, we have recently demonstrated their superior performance as heterogeneous catalysts for synthesis of testosterone derivatives[7] and CO_2 capture capacity as fluidized hybrid sorbents (also called *Flying MOFs*) for post-combustion flue gas of these hybrid MOF/MPM materials compared to the 'state-of-the-art'[8], as well as other very interesting applications currently undergoing in our group.

[a] *Address here.*
[b] *Address here.*
[c] *Address here.*
† Footnotes relating to the title and/or authors should appear here.
Electronic Supplementary Information (ESI) available: [details of any supplementary information available should be included here]. See DOI: 10.1039/x0xx00000x

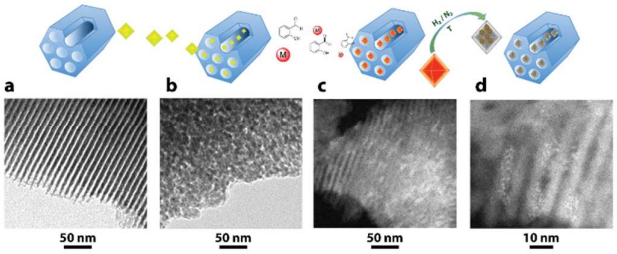

Figure 1. General approach for single MOF nanocrystal to single nanostructured catalyst transformation. TEM images for (a) SBA-15 and (b) (Zr)UiO-66(NH_2)/SBA-15. STEM images for (c) PdCl-SI-(Zr)UiO-66(NH_2)/SBA-15 and (d) Pd^0/SI-(Zr)UiO-66(NH_2)/SBA-15

Herein, we demonstrate that those supported and well-dispersed MOF nanocrystals can be used as optimal precursor for preparing either nanostructured mono- or bi-metallic metal oxides via transformation of *single MOF nanocrystal to single-nanostructured catalyst* within the mesoporous voids, which can be done upon 1) pyrolysis under nitrogen (from 400 to 1000 °C), 2) calcination under oxygen (400-800 °C) or 3) chemical reduction under hydrogen (from room temperature to 200 °C). This approach allows to preserve the initial 3D distribution of the MOF precursors along the cavities of the mesoporous material on the resulting nanostructured catalysts, thus avoiding the tendency of nanocrystals to fuse into larger crystallites[9], which is one of the major causes of loss of available active sites for supported catalysts. Therefore, stable and catalytically active nanometric catalysts have been prepared by our general strategy and tested for some catalytic reactions of potential interest, such as hydro-/dehydrogenation of novel Solid Organic Hydrogen Carriers (SOHCs).

Bimetallic nanostructured catalysts have been prepared by performing an additional multistep post-synthesis modification (PSM) of the MOF precursors before transformation, which consists in a gas-phase functionalization[10] followed by a selective metalation[11] (see Figure 1 and Scheme 1). As a showcase, here is described the preparation of PdCl-SI-(Zr)UiO-66(NH_2) nanocrystals confined within mesoporous silicas (such as SBA-15 or silica(A)) as precursor for their transformation into bimetallic nanostructured catalysts within mesoporous materials.

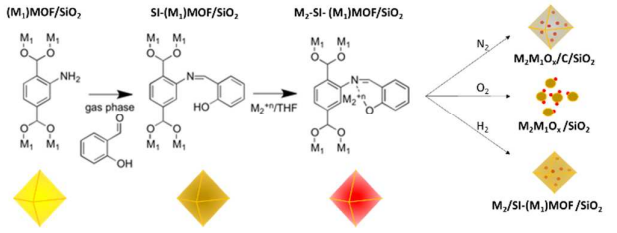

Scheme 1. General preparation of M_2-SI-(M_1)MOF-NH_2/SiO_2 as precursor for bimetallic nanostructured catalysts upon the possible transformation routes: pyrolysis under nitrogen, calcination under oxygen or reduction under hydrogen.

As shown in Scheme 1, a selective PSM of the free amino groups located at the ligands of (Zr)UiO-66(NH_2) was carried out via gas-phase treatment with salicylaldehyde vapor at 100 °C to convert amino groups into a salicylidenimine chelating ligands (SI). Subsequently, Pd was selectively chelated to the resulting Schiff base by soaking the solid material in a solution containing the metal salt $PdCl_2(CH_3CN)_2$ in THF. The faster functionalization and metal chelation rates visually observed for MOF hybrids compared to bulk MOFs are mainly due to the smaller particle size and excellent dispersion of the MOF nanocrystals within mesoporous silicas. It is noteworthy to mention that lower functionalization rates were also observed for MOF nanocrystals confined within SBA-15 with 9 nm monodimensional channels than for Silica(A), which is a mesoporous silica exhibiting tridimensional 30 nm in average non-regular cavities. MOF loadings below 20 wt.% were selected to provide sufficient initial spacing between MOF nanocrystals, since higher MOF loadings (20-40 wt.%) may lead to shorter distances between crystallites, and thereby, higher tendency to form aggregates during the transformation treatment. As an example of the available transformation steps, PdCl-SI-(Zr)UiO-66(NH_2)/SBA-15 was exposed to three different conditions : pyrolysis under nitrogen, calcination under oxygen or reduction under hydrogen. The resulting nanostructured catalyst are shown in Figure 2

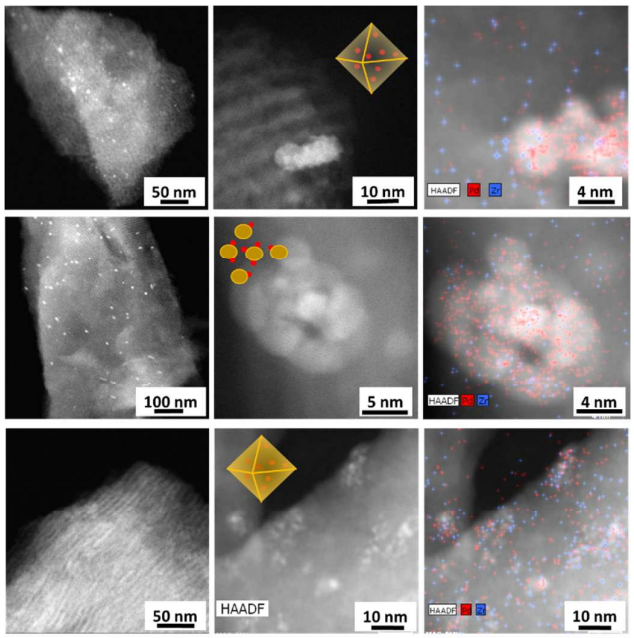

Figure 2. STEM-HAADF images and EDS for PdCl-SI-(Zr)UiO-66(NH_2)/SBA-15 treated under the three available transformation condition: (up) pyrolysis under nitrogen at 650 °C, (middle) calcination under oxygen at 500 °C, or (down) reduction under hydrogen at 200 °C. Pd (red dots) and Zr (blue dots) in EDS images.

Bimetallic nanostructured catalysts blended with carbonaceous species are typically obtained when the transformation is carried out under nitrogen at temperatures ranging from 500 to 900 °C. Nevertheless, TGA and elemental analysis data reveals that the complete 'de-carbonization' of MOF nanocrystals leading to naked Pd-ZrO_2 bimetallic nanostructured catalysts takes place for temperatures of pyrolysis above 900 °C compared to bulk MOF, in which microporous carbonaceous structures are remaining upon this treatment[3, 12]. Pyrolysis at lower temperature (<700 °C) can be used to avoid the complete carbon release from the

nanostructured catalysts, as revealed by TGA analysis (see Figure S3). According to TGA, all organic composition of the precursor is released at lower temperatures when air is used for the transformation (see Figure S3). Therefore, naked Pd-ZrO_2 bimetallic nanostructured catalysts are obtained for temperatures between 300-500 °C[13]. On the other hand, the transition metal cations decorating the MOF nanocrystal are reduced to form a monometallic Pd nanocrystals confined within the microporous cavities of the MOF when the transformation is carried out under hydrogen at milder temperatures (from room temperature to 200 °C), as shown in Figure 2. In this latter case, MOF structure is not decomposed and act as hosting matrix to stabilize nanometric Pd nanocrystals, as previously seen for Pd precursors confined within UiO-66[14]. This general approach can be extended to other bimetallic as well as monometallic MOF nanocrystals (see Table S1 and Figure S4 for some more examples).

To illustrate an example of the wide application of the resulting materials by taking advantage of their unique features, we have studied them as catalytically active platform for a pioneer concept of hydrogen storage system (see Figure S5), Fluidized-Nanoreactor Hydrogen Carriers (herein FNHCs), which consists in Solid Organic Hydrogen Carriers (herein, SOHCs) impregnated on nanostructured catalyst confined within fluidized mesoporous silica (herein, Fluidized-Nanoreactors, FN). SOHCs consist on the chemical hydrogen storage by binding H_2 to hydrogen-lean molecules by catalytic hydrogenation reactions, which can release that binded-H_2 via catalytic dehydrogenation to be used as fuel for several applications, ranging from realistic 'off-board' hydrogen filling stations to futuristic 'on-board' hydrogen generation on mobile platforms, such as in cars or space ships[15, 16].

In order to evaluate this concept, 33 wt.% of N-ethylcarbazole (**C**) was impregnated on 1.7 wt.% Pd/ZrO_2/Silica(A) prepared from PdCl-SI-UiO-66(NH_2)/Silica(A) treated at 900 °C under nitrogen. The resulting hydrogen-lean FNHC (H_0-FNHC) was loaded into a Parr bomb reactor and pressurized to 800 psig with H_2 at room temperature. The reactor was heated up to 220 °C and held until the pressure decreased and subsequently stabilized, thus indicating the end of the hydrogenation step (see Figure 3). An aliquot (5mg) of hydrogen-loaded FNHC (H_x-FNHC) was analyzed by extracting the H_2-loaded N-ethyl carbazole (H_x-C) with $CHCl_3$ and analyzed on a GC. Complete hydrogenation of H_0-C to H_x-C containing 93.0 % of H_{12}-C, 3.6 % of H_6-C and 3.4 % of H_4-C, according to GC analysis. In order to prove the reversibility, the H_x-FNHC was pressurized at 30 psig of H_2 and heated up to 220 °C holding until the pressure increased and was stabilized, which indicates the end of the dehydrogenation step. The analysis of the H_2-unload OHC extracted from the FNHC revealed 74.3 % of complete dehydrogenated compound (H_0-C) blended with remaining 22 % of H_6-C and 3.7% of H_{12}-C.

Subsequent hydro-dehydrogenation cycles revealed a significant loss of the H_2 storage-release reversibility due to the evaporation of the OHCs at the temperatures of operation condensing at the colder parts (tubing and valves) of the top Parr bomb reactor. This evaporation issue implies a major

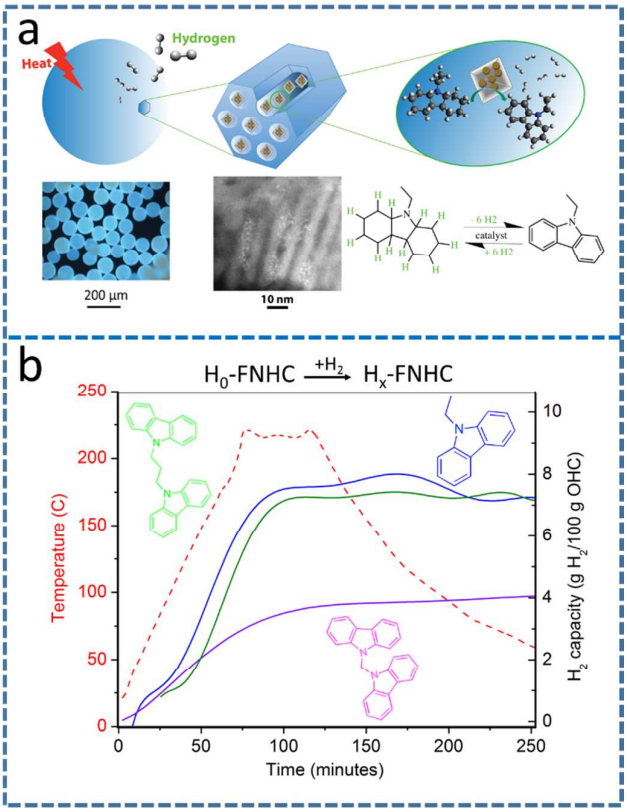

Figure 3. a) Pioneer concept of Fluidized-Nanoreactor Hydrogen Carriers (FNHCs) prepared via transformation of single MOF nanocrystals into single nanostructured catalyst within mesoporous supports. b) Hydrogenation kinetics of three different FNHCs containing N-ethylcarbazole (blue), bis(carbazol-9-yl)methane (violet) or 1,3-bis(carbazole-9-yl)propane (green). Temperature profile (red dashed line).

limitation for the implementation of FNHCs technology (see Figure S9 and S10), as well as it has been for LOHCs[17]. To design more efficient FNHCs as an early-stage alternative to conventional Liquid Organic Hydrogen Carriers (LOHCs) for 'on-board' H_2 supply, this main limitation must be addressed. Therefore, SOHCs have been synthetized and impregnated on the FN, that is, biscarbazoles (C_2X) with different N-substituted linkers (X), such as methyl and propyl (see Figure S6 and S7). The melting and boiling point of those biscarbazoles can be drastically changed by selecting the proper linker (X), which can vary from 61 °C and 250 °C for propyl (Pr) to 254 °C and 275 °C for methyl (Me), respectively, according to a TGA analysis (See Figure S8)[18]. Elevated boiling points can avoid the evaporation of the OHCs during the hydro-/dehydrogenation cycling. The impregnation of these compounds on 1.7 wt.% Pd/ZrO_2/Silica(A) (FN) was carried out by combining both solids together in a close glass ampoule under vacuum at 260 °C due to the low solubility of these compounds in any organic solvent.

The resulting FNHCs were tested for hydro/dehydrogenation and compared to the results obtained with the FNHC containing N-ethylcarbazole. Similar hydrogenation rate and H_2 capacity was measured for PrC_2 compared to **C**, up to 7 wt% of H_2 was stored on the SOHCs. To

the best of our knowledge, this is the first time that solid OHCs have been proposed due to their solid state at mild temperatures (below 40-50 °C) which avoids their application as liquid OHCs. Nevertheless, the dehydrogenation process was incomplete, since only up to 3.5 wt.% H_2 was released, as seen for **C** (See Figure S9). According to the GC analysis, volatile species are formed, which are attributed to hydrogenated N-propylcarbazole and carbazole molecules produced from the cleavage of **C_2Pr** during the hydrogenation step. Although **C_2Pr** was found unstable, the hydrogenation of **C_2Me** did not show evidences of evaporated species indicating more chemical stability under these specific conditions. Nevertheless, **C_2Me** having a melting point much higher than **C_2Pr** led to lower H_2 capacity due to its lower mobility within the mesoporous cavities of the silica support (see Figure 3), which may reduce its accessibility to the dispersed Pd active sites. Similar results to **C_2Me** were measured for poly(9-vinylcarbazole)-based FNHC, as showcase for non-mobile SOHC. Although the active metal sites dispersion is up to 6 times larger (see Figure S11), FNHCs obtained by H_2 reduction of PdCl-SI-(Zr)UiO-66(NH_2)/Silica(A) at 200 °C showed much lower activity due to the steric hindrance of bulky SOHCs to diffuse through (Zr)UiO-66-NH_2 pore apertures and to react with the active Pd nanocrystals confined within the MOF cavities[14].

Despite our attempts, alternative solid OHCs with elevated boiling points must be developed, such as **C_2Me** and **C_2Pr**, but exhibiting superior chemical stability through the hydro/dehydrogenation cycling and sufficient mobility within the mesoporous cavities to make viable a future technology using FNHCs. This pioneer concept for H_2 storage is bridging the gap between Hydrides of Light-weight Elements (HLEs) and Liquid Organic Hydrogen Carriers (LOHCs) combining the best of both worlds, since FNHCs can release hydrogen upon applying heat without the limitations of HLEs, such as safety concerns or non-reusability, while overcoming the inefficient release of hydrogen observed for the current 'on-board' catalytic packed bed reactors used on LOHC technologies, which suffer of poor contact between LOHCs and solid catalytic sites. FNHCs can be further optimized to meet the DOE's target for system-based H_2 storage dispositive (5.5 wt.% H_2 and 40 Kg m^{-3}, see Figure S5) by selecting an ideal hybrid system consisting of: 1) a multifunctional fluidized porous solid allowing up to 80-90 wt.% SOHCs loading and 1-1.2 g/mL of density, 2) confining highly stable solid SOHCs, and 3) containing minimum amount of highly active catalytic species dispersed within the pores[16].

Our general approach provides a precise control and versatility over the composition and structure of the MOF nanocrystalline precursor confined within mesoporous materials, which gives rise different nanostructured catalyst upon the selected transformation conditions and metal or metal oxide on the MOF SBUs for monometallic catalysts. Furthermore, bimetallic nanostructured catalysts can be prepared by the post-synthesis modification with chelating ligands and the subsequent incorporation of a second metal site in MOFs exhibiting free amino groups. These nanostructured catalysts confined within mesoporous materials have been applied in a pioneer concept of Fluidized-Nanoreactor Hydrogen Carriers.

References

1. K. J. Lee, J. H. Lee, S. Jeoung and H. R. Moon, Accounts of Chemical Research, 2017.
2. H. Liu, S. Zhang, Y. Liu, Z. Yang, X. Feng, X. Lu and F. Huo, Small, 2015, 11, 3130-3134; S. J. Yang, T. Kim, J. H. Im, Y. S. Kim, K. Lee, H. Jung and C. R. Park, Chemistry of Materials, 2012, 24, 464-470.
3. M. Y. Masoomi and A. Morsali, Coordination Chemistry Reviews, 2012, 256, 2921-2943.
4. L. Oar-Arteta, T. Wezendonk, X. Sun, F. Kapteijn and J. Gascon, Materials Chemistry Frontiers, 2017, 1, 1709-1745.
5. L. C. Liu, U. Diaz, R. Arenal, G. Agostini, P. Concepcion and A. Corma, Nature Materials, 2017, 16, 132-138.
6. I. Luz, M. Soukri and M. Lail, Chemistry of Materials, 2017, 29, 9628-9638.
7. F. G. Cirujano, I. Luz, M. Soukri, C. Van Goethem, I. F. J. Vankelecom, M. Lail and D. E. De Vos, Angewandte Chemie International Edition, 2017, 56, 13302-13306.
8. I. Luz, M. Soukri and M. Lail, Chemistry-A European Journal, 2018 (doi.org/10.1002/chem.201800612); I. Luz, M. Soukri and M. Lail, Chemical Science, 2018, 9, 4589-4599.
9. G. Prieto, J. Zecevic, H. Friedrich, K. P. de Jong and P. E. de Jongh, Nature Materials, 2013, 12, 34-39.
10. M. Servalli, M. Ranocchiari and J. A. Van Bokhoven, Chemical Communications, 2012, 48, 1904-1906.
11. X. Zhang, F. X. Llabrés i Xamena and A. Corma, Journal of Catalysis, 2009, 265, 155-160.
12. J. Tang, R. R. Salunkhe, H. Zhang, V. Malgras, T. Ahamad, S. M. Alshehri, N. Kobayashi, S. Tominaka, Y. Ide, J. H. Kim and Y. Yamauchi, Scientific Reports, 2016, 6, 30295; T. A. Wezendonk, V. P. Santos, M. A. Nasalevich, Q. S. E. Warringa, A. I. Dugulan, A. Chojecki, A. C. J. Koeken, M. Ruitenbeek, G. Meima, H. U. Islam, G. Sankar, M. Makkee, F. Kapteijn and J. Gascon, ACS Catalysis, 2016, 6, 3236-3247.
13. W. Cao, W. Luo, H. Ge, Y. Su, A. Wang and T. Zhang, Green Chemistry, 2017, 19, 2201-2211.
14. I. Luz, C. Rösler, K. Epp, F. X. Llabrés i Xamena and R. A. Fischer, European Journal of Inorganic Chemistry, 2015, 2015, 3904-3912.
15. P. Preuster, C. Papp and P. Wasserscheid, Accounts of Chemical Research, 2017, 50, 74-85.
16. T. He, P. Pachfule, H. Wu, Q. Xu and P. Chen, Nature Reviews Materials, 2016, 1, 16059.
17. Q.-L. Zhu and Q. Xu, Energy & Environmental Science, 2015, 8, 478-512; T. He, Q. Pei and P. Chen, Journal of Energy Chemistry, 2015, 24, 587-594; A. Bourane, M. Elanany, T. V. Pham and S. P. Katikaneni, International Journal of Hydrogen Energy, 2016, 41, 23075-23091; D. Teichmann, W. Arlt, P. Wasserscheid and R. Freymann, Energy & Environmental Science, 2011, 4, 2767-2773.
18. E. Asker and F. Filiz, Journal of Molecular Structure, 2013, 1040, 65-74.

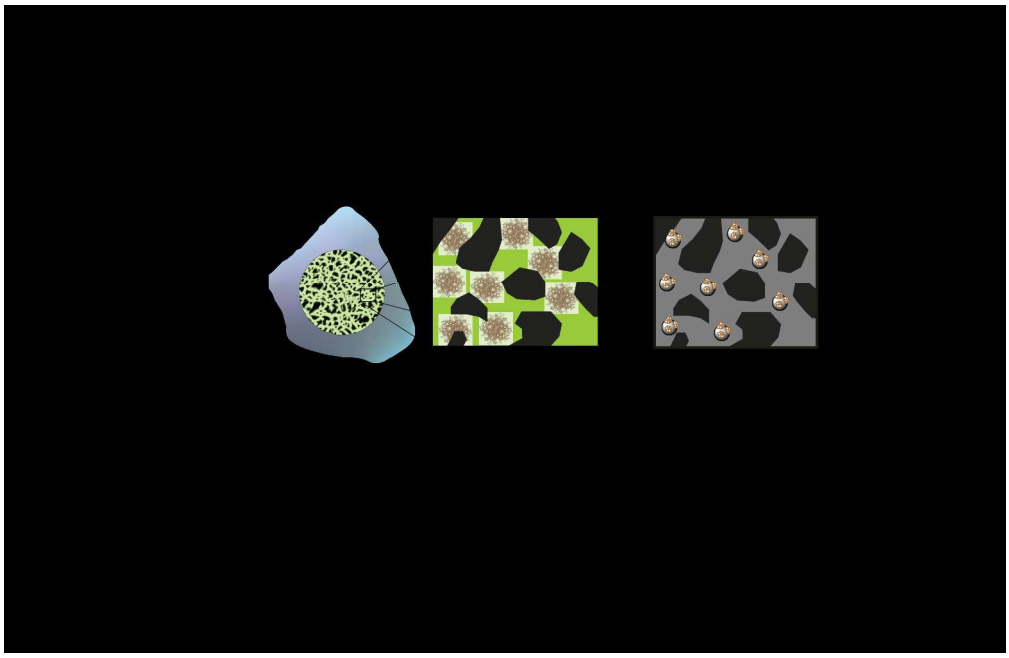

1763x1141mm (72 x 72 DPI)